Vacancy Solution Theory for Binary Adsorption Equilibria in Heterogeneous Carbon

L. P. Ding and S. K. Bhatia
Dept. of Chemical Engineering, The University of Queensland, Brisbane, Qld. 4072, Australia

A heterogeneous modified vacancy solution model of adsorption developed is evaluated. The new model considers the adsorption process through a mass-action law and is thermodynamically consistent, while maintaining the simplicity in calculation of multicomponent adsorption equilibria, as in the original vacancy solution theory. It incorporates the adsorbent heterogeneity through a pore-width-related potential energy, represented by Steele's 10−4−3 potential expression. The experimental data of various hydrocarbons, CO_2 and SO_2 on four different activated carbons — Ajax, Norit, Nuxit, and BPL — at multiple temperatures over a wide range of pressures were studied by the heterogeneous modified VST model to obtain the isotherm parameters and micropore-size distribution of carbons. The model successfully correlates the single-component adsorption equilibrium data for all compounds studied on various carbons. The fitting results for the vacancy occupancy parameter are consistent with the pressure change on different carbons, and the effect of pore heterogeneity is important in adsorption at elevated pressure. It predicts binary adsorption equilibria better than the IAST scheme, reflecting the significance of molecular size nonideality.

Introduction

Over the past several decades the subject of adsorption equilibrium has received considerable attention, and continues to do so in modern studies. The accurate representation of single-component adsorption equilibrium is a prerequisite for understanding multicomponent adsorption equilibria and adsorption kinetics. Moreover, adsorption of simple compounds has become an effective way for characterization of porous materials used in industrial processes. While developments in transmission electron microscopy and other methods with molecular-scale resolution make it possible to visualize the microporous structure, quantitative representation of the structure from such visualizations is a complex task. For this reason characterization of porous solids through adsorption-related methods is still the most popular technique. Nevertheless, the wide variety of compounds used in practice, such as argon, nitrogen, and hydrocarbons, often leads to difficulties in obtaining consistent results because of the different physical and chemical properties of the adsorbates used.

The approaches for adsorption equilibrium studies can be broadly classified under two categories, those based on classic continuum modeling and those based on molecular theories. Generally, the classic method attempts to describe the adsorption equilibrium with an isotherm equation containing a small number of parameters. At a minimum, these parameters include the extent of the surface, such as the monolayer capacity and the molar intensity of the gas–surface interaction. The Langmuir isotherm (Langmuir, 1918) is one of the most popular choices for single-component adsorption on homogeneous surfaces over low to moderate operating pressure. Although it was initially based on the mechanism of dynamic equilibrium between the adsorption and desorption processes, it can also be derived from statistical thermodynamics (Fowler and Guggenheim, 1949). There have been numerous modifications of the Langmuir equation to take into account effects such as lateral interaction between adsorbate molecules and the nonuniformity of the surface (Yang, 1997).

The molecular theory method for adsorption has grown rapidly in recent years with developments in computation hardware and software. It can be generally divided into molecular-based statistical thermodynamic theory methods and molecular simulation methods. The density functional theory (DFT) is a method based on statistical thermodynam-

Correspondence concerning this article should be addressed to S. K. Bhatia.

ics, while the grand canonical Monte Carlo method (GCMC) is an accurate simulation approach. Although these methods can provide accurate solutions for adsorption of simple molecules in model pores (Olivier, 1995; Davies and Seaton, 1999), the extension to complex molecules and to adsorbents with disordered microstructure is still a challenge for researchers.

Physical adsorption of gases and vapors has been a useful method for characterization of microporous carbonaceous adsorbents. For this purpose, the adsorption equilibrium is expressed by a generalized adsorption isotherm (GAI), with the local isotherm integrated over a heterogeneity such as pore-size distribution. One approach that is commonly employed by researchers interested in pore structure is the Dubinin's equation and expressions (Jaroniec et al., 1988) originating from it. Although it is not thermodynamically consistent in the Henry's law limit, it is mathematically simple because of the direct correlation of its energy parameter with the pore width (McEnaney, 1987).

The prediction of binary adsorption equilibria on porous adsorbents, such as activated carbon, has been a challenge for many studies. While the ideal adsorbed solution theory (IAST) method (Myers and Prausnitz, 1965) has set up the foundation for prediction of multicomponent equilibria from single-component isotherms, the extension of classic isotherms, such as the extended Langmuir equation, is often a simpler alternative. However, the latter methods require validation of thermodynamic consistency, and several popular models, such as the extended Langmuir equation, either fail consistency tests or are consistent only under restrictive conditions (Rao and Sircar, 1999). Among these is also the vacancy solution theory (VST) of Suwanayuen and Danner (1980a,b) and Cochran et al. (1985a), which was shown to predict inconsistent binary selectivity in the Henry's law limit (Talu and Myers, 1988). Nevertheless, while thermodynamically consistent, the IAST is known (Sircar, 1995) to be inaccurate in the presence of size nonideality, and is computationally cumbersome in the presence of heterogeneity. Thus, there is considerable need for a thermodynamically consistent heterogeneous isotherm that has single- and multicomponent forms within a common framework.

The more rigorous molecular simulation method has been applied to binary adsorption of simple molecules on activated carbon (Gusev and O'Brien, 1998; Davies and Seaton, 1999, 2000). The DFT method has also been extended to binary adsorption of small molecules (Kierlik and Rosinberg, 1991; Somers et al., 1993; Bhatia, 1998). However, the computation time required prevents its routine use for process-design purposes and for complicated molecules, or in the presence of heterogeneity.

In an effort to correct the existing VST we have recently (Bhatia and Ding, 2001) proposed a new derivation of this theory, utilizing a mass-action principle, that can provide thermodynamically consistent multicomponent isotherms. While the new theory is general enough to accommodate any arbitrary activity coefficient model, the particular case of the Flory-Huggins model leads to the multisite Langmuir model of Nitta et al. (1984), which is known to be thermodynamically consistent (Rao and Sircar, 1999). The single-component form of this model has also been extended to the heterogeneous case and successfully incorporated into a model of adsorption kinetics in bidisperse carbons (Ding et al., 2001). This article investigates the characterization of activated carbons by the heterogeneous VST, and the subsequent prediction of multicomponent isotherms on the same carbon over a wide range of conditions. Data in the literature for four different carbons are interpreted in this way, and it is seen that use of the approach provides successful predictions of binary equilibrium for a variety of hydrocarbons and carbon dioxide.

Theory

The vacancy solution theory, developed two decades ago by Suwanayuen and Danner (1980a,b) using the Wilson activity expression, and later reformulated by Cochran et al. (1985a,b) using the Flory–Huggins activity coefficient relations, provides an expression for both single- and multicomponent adsorption equilibrium in the same framework, and therefore simplifies the calculation for mixture adsorption. However, this method has not been widely accepted and utilized in research and practice, possibly because it contradicts thermodynamic consistency under some circumstance (Talu and Myers, 1988). Another shortcoming of this method is that the heterogeneity of the adsorbent has not been considered in the models, therefore it cannot be reliably applied to adsorption in disordered microporous materials. In this work, the adsorption process is analyzed in a more general way than the original treatment (Suwanayuen and Danner, 1980a,b; Cochran et al., 1985a) by considering the stoichiometry

$$A_i(g) + \nu_i V(a) \Leftrightarrow A_i(a). \tag{1}$$

Here $A_i(a)$ is the adsorbate of species i, V represents the vacant site, and ν_i is the number of vacant sites occupied by a molecule of adsorbate i. It has been shown (Ding and Bhatia, 2001) that ν_i plays a significant role in the modified vacancy solution theory, and the original Flory–Huggins model-based vacancy solution theory (Cochran et al., 1985a) was developed under the assumption of $\nu_i = 1$.

Modified vacancy solution theory

Using the mass-action principle, the equilibrium condition of Eq. 1 can be represented by

$$\frac{X_i^a \gamma_i^a}{\left(X_\nu^a \gamma_\nu^a\right)^{\nu_i}} = \phi_i^g y_i P \exp\left(-\frac{\Delta G_i^0}{R_g T}\right), \tag{2}$$

in which the adsorbed phase is considered as a solution of vacancies and adsorbed molecules. The mole fraction of species i can be represented by

$$X_i^a = \frac{n_i}{n_T}, \quad i = 1, \ldots, N, \nu \tag{3}$$

in which n_i is the adsorbed amount of species i, and

$$n_T = n_\nu + \sum_{j=1}^{N} n_j \tag{4}$$

is the total amount of adsorbate and vacancies at equilibrium. A balance over the vacancy species yields

$$n_{\nu\infty} = n_\nu + \sum_{j=1}^{N} \nu_j n_j, \tag{5}$$

which combines with Eqs. 3 and 4 to provide

$$X_i^a = \frac{n_i}{n_{\nu\infty} - \sum_{j=1}^{N} (\nu_j - 1) n_j} \tag{6}$$

and

$$X_\nu^a = \frac{n_{\nu\infty} - \sum_{j=1}^{N} \nu_j n_j}{n_{\nu\infty} - \sum_{j=1}^{N} (\nu_j - 1) n_j}. \tag{7}$$

Here $n_{\nu\infty}$ is the maximum vacancy concentration. The activity coefficients γ_i^a and γ_ν^a can be written by different thermodynamic expressions, such as the Wilson equation and Flory–Huggins equation. In this work we utilize the Flory–Huggins model in the form

$$\ln(\gamma_i^a) = 1 - \ln\left[\sum_{j=1}^{N} \frac{X_j^a}{(1+\alpha_{ij})}\right] - \left[\sum_{j=1}^{N} \frac{X_j^a}{(1+\alpha_{ij})}\right]^{-1}, \quad i = 1, \ldots, N, \nu. \tag{8}$$

This is a particularly convenient choice of activity coefficient model over other expressions, because the Flory–Huggins interaction parameter $(1+\alpha_{i\nu})$ represents the ratio of molecular area to vacancy area, and can be directly related to the site occupancy ν_i.

The equilibrium constant $e^{-(\Delta G_i^0/R_gT)}$ in Eq. 2 can be related to the Henry's law coefficient by considering the limit $X_i^a \to 0$ and $X_\nu^a \to 1$ for $P \to 0$, which yields

$$K_i = \frac{R_g T n_{\nu\infty} e^{a_{i\nu}} e^{-(\Delta G_i^0/R_gT)}}{1+\alpha_{i\nu}}, \quad i = 1, \ldots, N. \tag{9}$$

Substituting the preceding result into Eq. 2, the modified vacancy solution model based on the Flory–Huggins activity coefficients is given by

$$\frac{X_i^a \gamma_i^a}{(X_\nu^a \gamma_\nu^a)^{\nu_i}} = \frac{(1+\alpha_{i\nu}) e^{-\alpha_{i\nu}}}{n_{\nu\infty} R_g T} K_i \phi_i^g y_i P, \quad i = 1, \ldots, N. \tag{10}$$

Both parameters ν_i and $(1+\alpha_{i\nu})$ represent the number of vacant sites occupied by one molecule of adsorbate i and must be equal to satisfy the requirement of thermodynamic consistency, so that we have

$$\nu_i = 1 + \alpha_{i\nu}. \tag{11}$$

The surface coverage for species i can be defined as

$$\theta_i = \frac{n_i \nu_i}{n_{\nu\infty}}. \tag{12}$$

Combining Eqs. 6–12, the final expression for the modified vacancy solution model can be obtained as

$$\frac{\theta_i}{\left(1 - \sum_{j=1}^{N} \theta_j\right)^{\nu_i}} = \frac{\nu_i K_i}{n_{\nu\infty} R_g T} \phi_i^g y_i P, \tag{13}$$

which is precisely the multisite Langmuir model of Nitta et al. (1984), and the thermodynamic consistency of this equation has already been verified (Rao and Sircar, 1999). The binary selectivity in the Henry's law limit becomes

$$\lim_{P \to 0} (S_{12}) = K_1/K_2, \tag{14}$$

regardless of the bulk composition, demonstrating that the revised theory does not suffer from the deficiency of the original VST pointed out by Talu and Myers (1988).

Incorporation of adsorbent heterogeneity

Equation 13 can be further extended to include the effect of structural heterogeneity of porous adsorbents. To this end the equilibrium constant can be related to the pore potential, following the established result for the Henry's law coefficient

$$K_i(H) = e^{-(\Phi_{\rm mi}(H)/R_gT)}, \tag{15}$$

where $\Phi_{\rm mi}(H)$ is the potential energy in a micropore of width H. Hence the local isotherm equation at a pore of width H can be obtained by substituting the preceding equation into Eq. 13, to obtain

$$\frac{\theta_i}{\left(1 - \sum_{j=1}^{N} \theta_j\right)^{\nu_i}} = \frac{\nu_i e^{-(\Phi_{\rm mi}(H)/R_gT)}}{n_{\nu\infty} R_g T} \phi_i^g y_i P. \tag{16}$$

The micropores in activated carbon are represented as a slitlike pore space confined between two parallel surfaces, that are separated by a distance H between centers of carbon atoms in the surface layers. Steele (1973) has developed the expression for the gas–solid interaction potential at this surface:

$$\phi_{is}(z) = 2\pi\rho_s \epsilon_{is} \sigma_{is}^2 \Delta \times \left[0.4\left(\frac{\sigma_{is}}{z}\right)^{10} - \left(\frac{\sigma_{is}}{z}\right)^4 - \frac{\sigma_{is}^4}{3\Delta(z+0.61\Delta)^3}\right]. \tag{17}$$

The potential energy within the slit pore is the sum of the contribution from the opposite walls, and is assumed to cor-

respond to the value at the potential minimum, leading to

$$\Phi_{\mathrm{mi}}(H) = \min\left[\phi_{is}(z) + \phi_{is}(H-z)\right]. \tag{18}$$

Here z is the distance of the adsorbate molecule from one of the pore walls and the distribution of the potential energy is symmetrical with respect to the middle of the pore.

The micropore-size distribution is expressed by a gamma distribution function to yield

$$f(H) = \frac{q^{\gamma+1}H^{\gamma}e^{-qH}}{\Gamma(\gamma+1)}. \tag{19}$$

The amount adsorbed for species i can then be calculated following the GAI

$$n_{t,i}(P,T) = V_p \frac{n_{\nu\infty}}{\nu_i}\int_0^{\infty}\theta_i(H,P,T)f(H)\,dH, \tag{20}$$

in which $\theta_i\,(H,P,T)$ is obtained from Eq. 16.

Solution Methodology and Application to Experimental Data

The experimental adsorption data of various adsorbates on four different activated carbons at multiple temperatures have been utilized and analyzed in order to test the applicability of the heterogeneous modified vacancy solution model just described. Initially, the single component data were fitted by the model equation and the parameters for the isotherm as well as pore-size distribution extracted from the model fitting. These values were then applied to predict binary adsorption equilibria on the same adsorbent under given conditions.

The adsorption data studied are those of hydrocarbons, CO_2 and SO_2 on Ajax carbon at various tempertures (Do and Wang, 1998), hydrocarbons on Norit carbon at three temperatures (Qiao et al., 2000), hydrocarbons and CO_2 on Nuxit carbon at four temperatures between 293 and 363 K (Szepesy and Illes, 1963a,b), as well as of hydrocarbons and CO_2 on BPL Calgon carbon at 260.2 K and 301.4 K under pressures up to 35 atomosphere (Reich et al., 1980).

For each carbon, all the single adsorption data are fitted simultaneously using a nonlinear least-square procedure to estimate the common parameters $n_{\nu\infty}$, q, and γ. Considering the effect of temperature on the capacity of the adsorbate, the following relation is assumed (Ding et al., 2001):

$$\nu_i = \nu_i^0\,\exp\left[\delta_i(T-T_0)\right], \tag{21}$$

where ν_i^0 is the vacancy occupancy of compound i at the reference temperature T_0, and δ_i is the thermal expansion coefficient for species i. The adsorbate-related fitting parameters are ν_i^0, δ_i, and ϵ_{is}. Here $\epsilon_{is} = 6/5\pi\rho_s\epsilon_{is}\sigma_{is}^2\Delta$ is the magnitude of the fluid–solid interaction potential well. The pairwise parameter σ_{is} is calculated by $\sigma_{is} = (\sigma_{ii}+\sigma_{ss})/2$ following the Lorentz rule. Because of the finite size of adsorbate molecules and the pore width H representing the distance between the centers of carbon molecules on the first layer of the opposite wall, there are some extremely small micropores excluded from the adsorbate molecules. Therefore, in the evaluation, the lower limit of integration in Eq. 20 is taken as $H_{i,\min}$ rather than 0. Here $H_{i,\min}$ is the species-related minimum accessible pore width in which the minimum of fluid–solid potential energy equals zero, that is, $\Phi_{\mathrm{mi}}\,(H_{i,\min}) = 0$. The fugacity coefficient ϕ_i^g in Eq. 16 is calculated by the Benedict–Webb–Rubin (BWR) equation of state (Assael et al., 1996).

With the isotherm parameters and pore-size distribution information obtained from the fitting of single-component adsorption data, binary adsorption equilibria on corresponding activated carbons are predicted from Eqs. 16 and 20. When the molecular sizes of the adsorbate pair are different, single-component adsorption will occur in micropores between the two sizes, and the single-component version of the heterogeneous modified vacancy solution model is utilized for such micropores. The two nonlinear algebraic equations representing local adsorption equilibrium for the adsorbate components are solved by a globally convergent Newton's method (Press et al., 1992). Further details of the computation and fitting procedure are available in our recent study (Ding and Bhatia, 2001), combining the single-component form of the original VST with heterogeneity.

Results

Adsorption on Ajax carbon

The single-component adsorption isotherms of C_2H_6, C_3H_8, n-C_4H_{10}, C_6H_6, C_7H_8, and SO_2 on Ajax carbon at various temperatures (Do and Wang, 1998) were first fitted by this model. The micropore volume of Ajax carbon is reported as 0.44 cm^3/g based on N_2 adsorption analysis (Do and Do, 1997). The fitting results for single-component adsorption equilibrium and micropore-size distribution of Ajax carbon have been displayed as the solid line in Figures 1 and 2, respectively. The values of the fitting parameters are listed in Table 1. It can be found from Figure 1 that the proposed model can successfully fit all the experimental data. The modal micropore size for this carbon is about 1 nm and the micropore sizes lie in the range of 0.55–1.6 nm, as shown in Figure 2.

The fitted isotherms using the heterogeneous unmodified VST model (Ding and Bhatia, 2001), which uses $\nu_i = 1$, on the same data are also presented in Figure 1, and the corresponding micropore-size distribution is presented in Figure 2, using dashed lines. Although the total number of fitting parameters of the unmodified heterogeneous VST model is more than that of the proposed model by $m-1$ (m is the number of species studied), the overall fitting result of the present model is slightly better than that of the heterogeneous VST model, indicating its superiority. This is particularly evident for the adsorption of SO_2 at three different temperatures. The original VST model is derived under the assumption of $\nu_i = 1$, implying that one adsorbate molecule can occupy one vacant site. In reality, a vacant site can be occupied by multiple molecules when the molecular size is very small compared with the vacancy size. In addition, for polar molecules like SO_2, there is molecular interaction resulting from the quadruple moment. Although the electrostatic force caused by the approach of two molecules de-

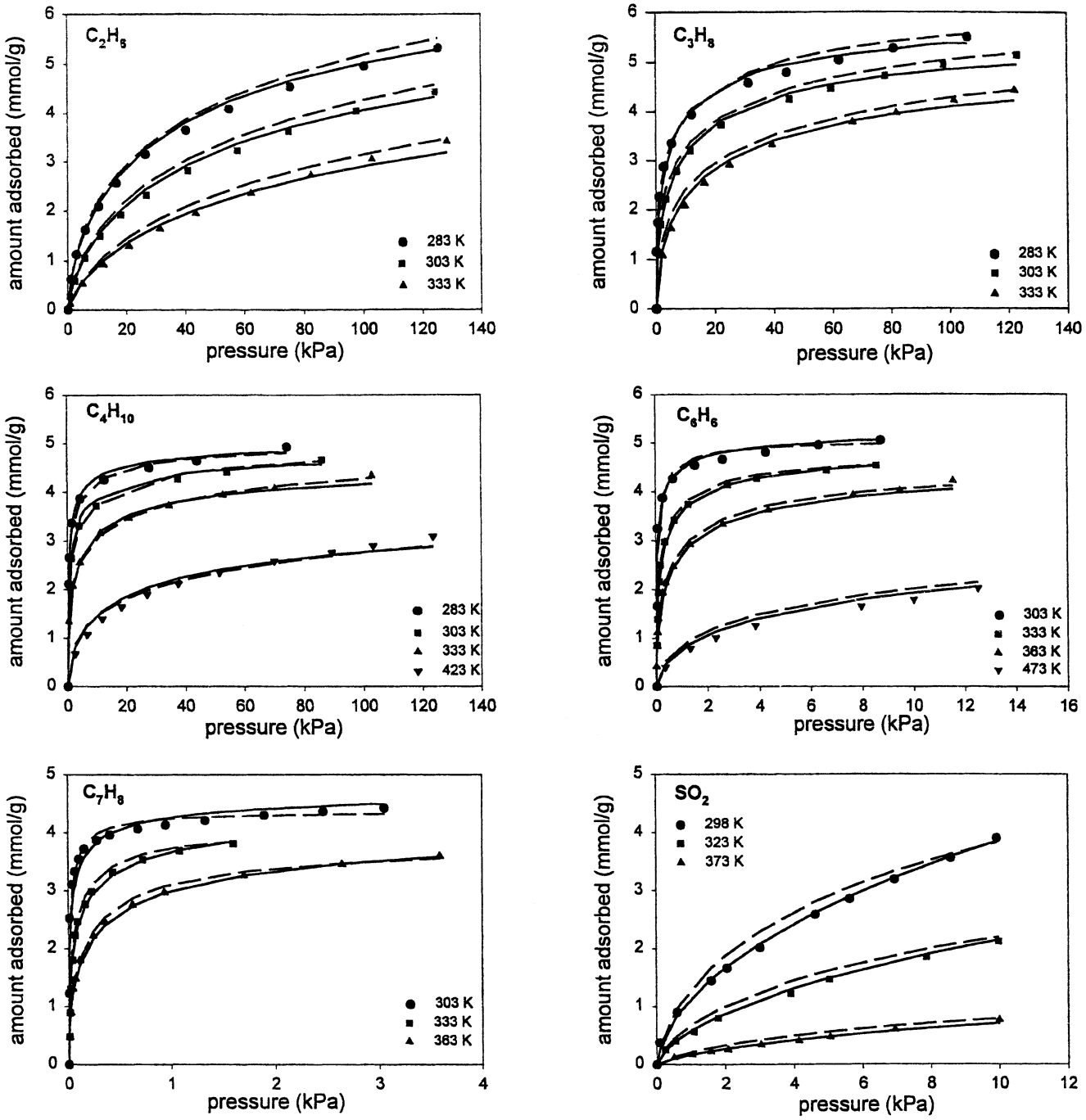

Figure 1. Adsorption isotherms on Ajax carbon.

Solid lines are the fitting results using the present model, and dashed lines are the fitting results from the heterogeneous unmodified VST model. Symbols are experimental data.

pends on the orientation and distance of the molecules, the net effect on the bulk properties of the fluid is an attractive force (Assael et al., 1996). From the adsorption point of view, this force can result in enhanced adsorption of the polar species over the one arising from the Lennard–Jones pairwise potential, reducing the effective value of ν_i. The application of Eq. 11 and ν_i as a fitting parameter overcomes the limitation of the original VST model, improving the fit of the experimental data.

As additional validation, the model was subsequently utilized to predict the single-component adsorption equilibrium of C_2H_6 and C_3H_8 at temperatures other than those in Figure 1, using the fitting parameters given in Table 1. In addition, data for CH_4 and CO_2 were fitted using the above PSD. For CH_4 and CO_2 the value of adsorbate-specific parameters ν_i^0, δ_i, and ϵ_{is} were obtained by fitting the experimental equilibrium data with the common parameters fixed from the earlier result. The predicted single-component adsorption

Table 1. Parameters for Different Adsorptives on Ajax Carbon

Adsorbate	σ_{ii} (nm)	$\delta_i \times 100$ (K^{-1})	ν_i^0	ϵ_{is} (kJ/mol)	q (nm^{-1})	γ	$n_{\nu\infty}$ (mmol/cm^3)
C_2H_6	0.39	0.334	1.203	11.663			
C_3H_8	0.43	0.167	1.487	14.303			
n-C_4H_{10}	0.43	0.132	1.768	17.758			
C_6H_6	0.37	0.157	1.648	25.073	39.75	39.43	20.93
C_7H_8	0.38	0.106	1.849	26.44			
SO_2	0.36	1.258	0.663	14.441			
CO_2	0.33	0.702	0.88	9.702			
CH_4	0.38	1.07	1.155	7.475			

Note: q, γ, and $n_{\nu\infty}$ are species-independent structural parameters.

isotherms are compared with the experimental results (Wang, 1998) and displayed in Figure 3 as the solid lines. The prediction is satisfactory for the adsorption of C_2H_6 and C_3H_8 at both 258 K and 273 K, supporting the correlation of ν_i with temperature and the reliability of the fitting parameters. The predicted results of CO_2 and CH_4 are also satisfactory, indicating that the extracted pore-size distribution is reliable. The unmodified heterogeneous VST model was also applied in the same manner and the results were displayed in Figure 3 by the dashed lines. This model can also predict the isotherm very well. Because the adsorbates are simple nonpolar hydrocarbons, and the experimental pressures are not high for CO_2 and hydrocarbons, the neglect of molecular size difference represented by ν_i has little effect on the overall fitting results. The original VST model does appear to predict the data a little better than the present model, particularly for adsorption of C_3H_8 at very low pressures. This is due to the larger number of fitting parameters involved and is not significant, as is evident from the better predictions of multicomponent equilibria based on the current approach, as discussed below.

The binary adsorption equilibrium of CH_4 with C_2H_6, C_3H_8, and CO_2 on Ajax carbon at the bulk pressure of 66.7 kPa was subsequently predicted using the single-component isotherm parameters and the micropore-size distribution extracted by the heterogeneous modified VST model. The predicted results represented by the solid lines along with the experimental data (Wang, 1998) are displayed in Figure 4. In addition, utilization of the single-component adsorption isotherm form of the present model (Eq. 16 with $N = 1$) in the IAST model (IAST-HMVST) was also used to predict binary adsorption equilibria. The predicted results are depicted in Figure 4 by the dotted lines, while the dashed lines represent the predicted adsorption equilibria by IAST with the heterogeneous unmodified VST isotherm (IAST-HVST). Among the three approaches, the present model gives the best-predicted result. Although the prediction of the IAST-HMVST model is acceptable in accuracy, the calculation time required is much more than that of the present model. For example, the calculation time of the present model for CH_4 and C_2H_6 adsorption is about 30 s using a PII 256 MB personal computer, while it takes 720 s using the IAST-HMVST model on the same machine. The deviation of the IAST-HVST predictions for C_2H_6 and C_3H_8 from the experimental data may be due to the overprediction of the HVST isotherm for single-component adsorption of these compounds at the corresponding pressure and temperature, as shown in Figure 1. The results demonstrate that the accurate representation of single-component adsorption equilibrium at the operating conditions is essential for the successful prediction of binary adsorption equilibria. A small deviation in the single-component adsorption equilibrium may cause considerable deviation in the binary case.

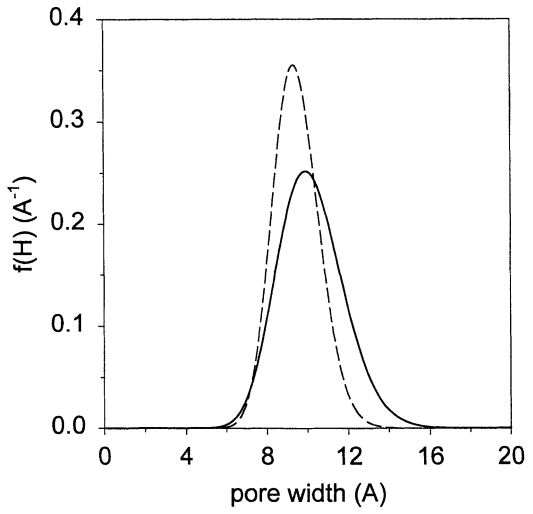

Figure 2. Micropore-size distribution of Ajax carbon extracted by different models.

Solid line is the PSD from the present model, and dashed line is that from the heterogeneous unmodified VST model.

Adsorption on Norit carbon

After the application to the Ajax carbon, the single-component adsorption equilibrium of CH_4, C_2H_6, and C_3H_8 on Norit carbon at 303 K, 333 K, and 363 K, respectively (Qiao et al., 2000), was fitted by this model. The micropore volume of Norit carbon is reported as 0.47 cm^3/g (Qiao et al., 2000). The solid line in Figures 5 and 6 represents the fitting results for single-component adsorption equilibrium and micropore-size distribution of Norit carbon, respectively. The values of the fitting parameters are listed in Table 2. For comparison, the heterogeneous unmodified VST model was also applied to the adsorption data on Norit carbon, and the fitting results are displayed in Figure 5 by the dashed lines.

As for the Ajax carbon, it is evident that the proposed model can successfully fit all the single-component adsorption data, as can the heterogeneous unmodified VST model. The modal micropore size for this carbon is about 1 nm, with the micropores lying in the 0.6–1.6 nm range, which is similar

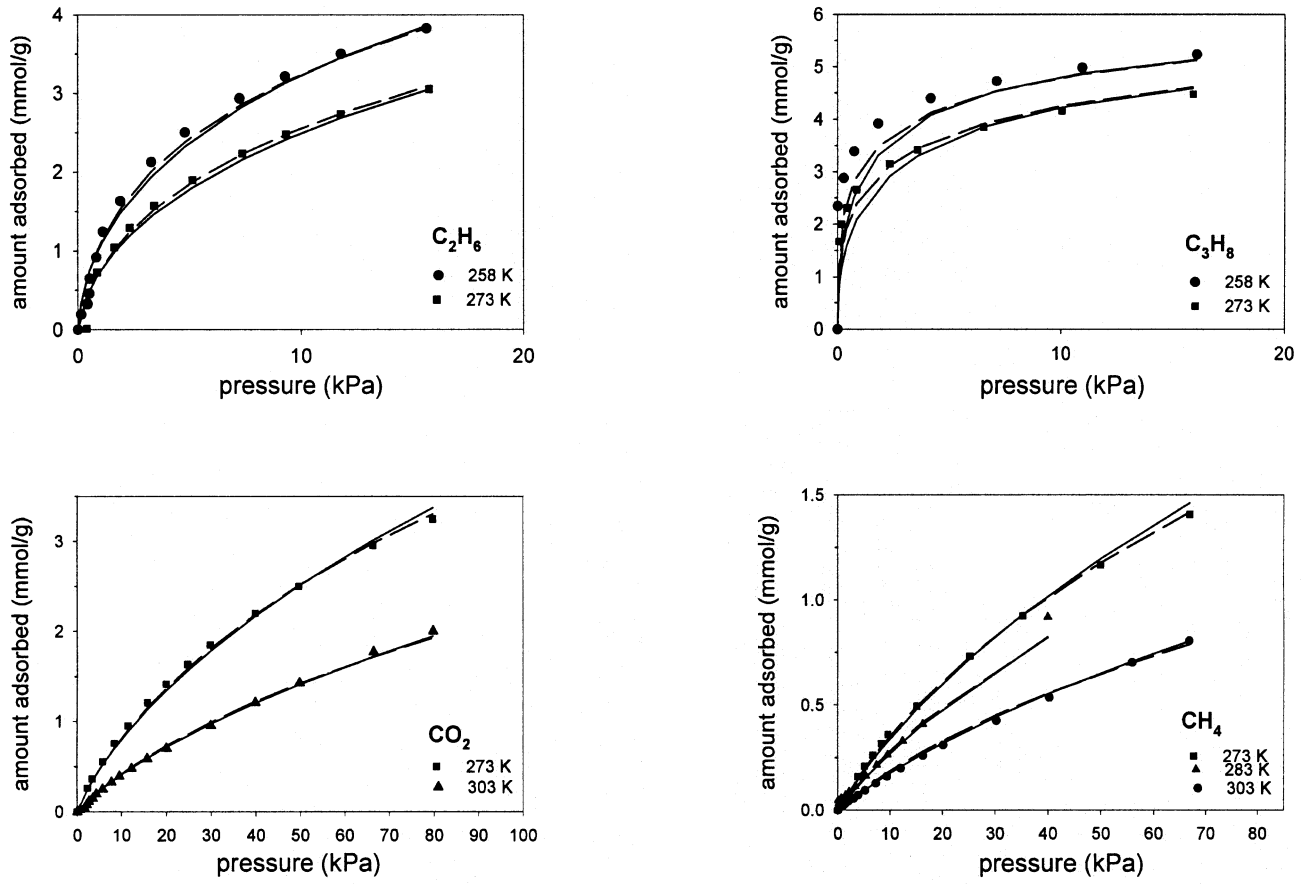

Figure 3. Predicted adsorption isotherms on Ajax carbon.

Solid lines are results from the present model, and dashed lines are results from the heterogeneous unmodified VST model. Symbols represent experimental data.

to the Ajax carbon. The micropore-size distribution extracted by the heterogeneous VST model is represented by the dashed line in Figure 6.

Following the single-component data fitting, binary adsorption equilibrium on Norit carbon at a total pressure of 50.6 kPa and three different temperatures was predicted, using the parameters from single-component adsorption isotherms. The results, represented by the solid lines, as well as pertinent experimental data (Qiao et al., 2000) are given in Figure 7. It is readily seen that the model can predict the binary adsorption equilibria of CH_4 and C_2H_6, CH_4, and C_3H_8 at different temperatures with reasonable accuracy. However, for C_2H_6–C_3H_8 mixtures, while prediction of the amount of C_2H_6 adsorbed is consistent with the experimental value, that for C_3H_8 is somewhat lower. For comparison, the single-component adsorption isotherms of each compound at the corresponding partial pressure, calculated by the single-component model, are plotted by the dash-dotted lines in Figure 7. It would appear that the existence of CH_4 has barely, if any, effect on the adsorption of the strongly adsorbed components C_2H_6 and C_3H_8, and for binary mixtures with CH_4 the isotherms for these two compounds overlap with the corresponding single-component isotherms. This can be easily explained, as both C_2H_6 and C_3H_8 have much stronger interactions with carbon than does CH_4, and these components are also substantially stronger than their interactions with CH_4, so the existence of CH_4 has little effect on their adsorption. On the other hand, the slight underprediction for CH_4 may be due to the stronger attractive interaction of the CH_4–C_2H_6 and CH_4–C_3H_8 pairs than the CH_4–CH_4 pair. Even more interesting is the result for the adsorption of C_3H_8 in the mixtures with C_2H_6. This clearly shows that for C_3H_8 the single-component isotherm coincides with the binary experimental data at all three temperatures, suggesting that C_3H_8 in the mixture is unaffected by C_2H_6. This is most likely due to the dominance of the C–C_3H_8 interaction, compared to the C_2H_6–C_3H_8 interaction. The latter is somewhat simplified in the model that ignores differences in attractive potential between the C_2H_6–C_2H_6 and C_3H_8–C_3H_8 pairs. This idealization strongly offsets the predictions for C_3H_8, as is evident from Figure 7. The results clearly indicate room for improvement of the model by considering improvements to the Flory–Huggins model, involving adsorbate interactions. Such interactions can be most simply incorporated in a mean-field sense by considering nearest-neighbor interactions, though for binary systems, exact results from the one-dimensional Ising model, and various approximations in higher dimensions also exist (Hill, 1960). We intend to investigate these aspects in our future work.

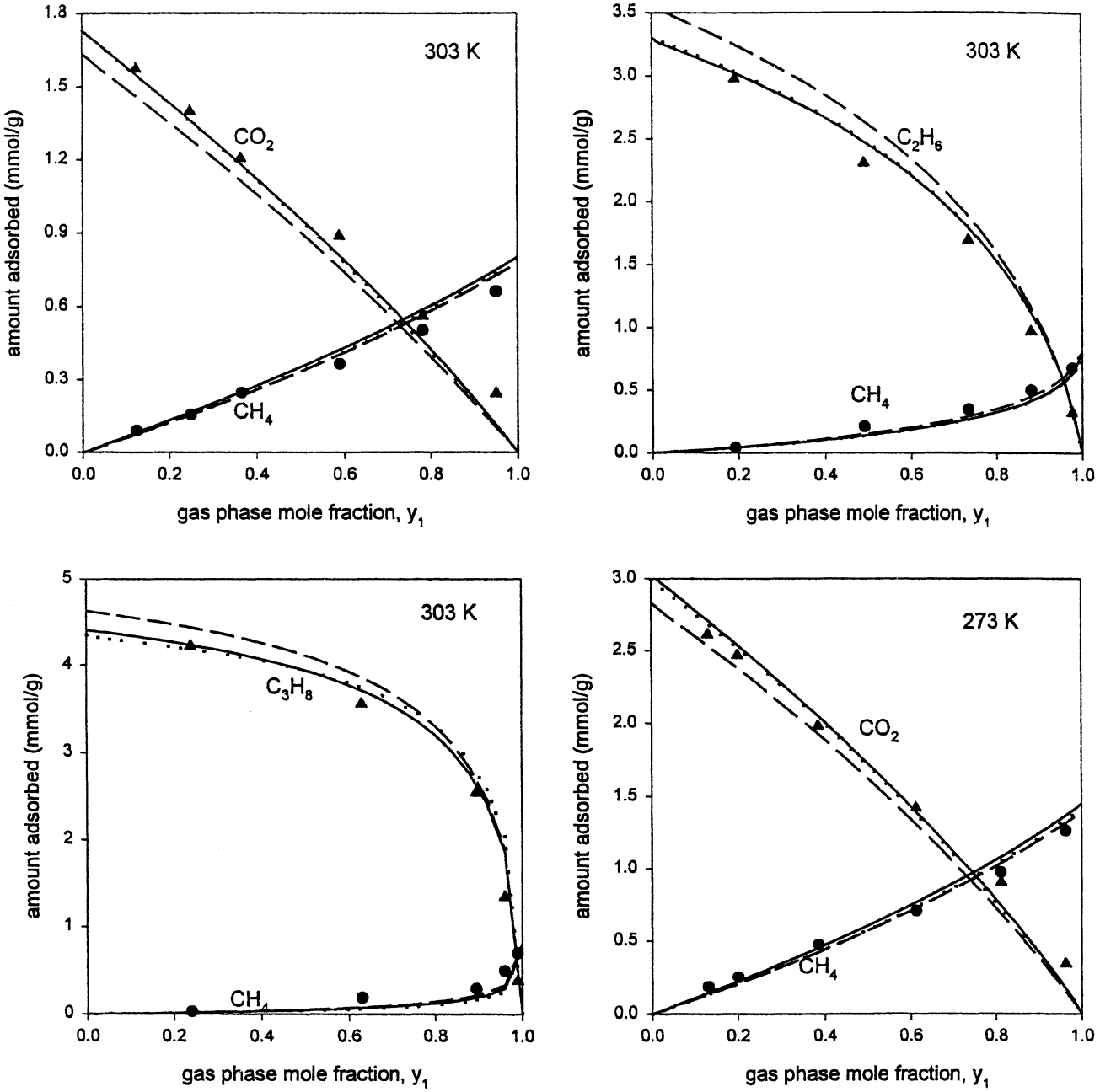

Figure 4. Prediction of binary adsorption equilibria on Ajax carbon at bulk pressure of 66.7 kPa by different models.

Solid lines are results using the present model, dotted lines are predictions using the IAST-HMVST model, and dashed lines are results of the IAST-HVST model. Symbols represent the experimental data.

It is also interesting to see that the amount of CH_4 adsorbed in the mixture with C_2H_6 and C_3H_8 at higher temperatures is the same as that adsorbed in the single-component case, which exceeds the prediction based on the solid–fluid interaction potential. The reason for this observation may be the interaction between the adsorbate molecules. The theoretical simulation as well as the experimental result have found plenty of evidence for this kind of behavior. The DFT simulation of adsorption on slit pores has found that the existence of a small amount of C_2H_6 and C_3H_8 can increase the adsorption of CH_4 (Bhatia, 1998). The molecular simulation calculation for CH_4 adsorption in slit-shaped pores from mixtures with C_2H_6 also indicates that at high CH_4 mole fraction (greater than 0.8), CH_4 adsorption is almost the same as in the single case for the pore range between 0.762 and 1.143 nm (Davies and Seaton, 1999). This phenomenon was also observed in the binary adsorption experiment of CH_4–C_3H_8 on activated carbon (Ahmadpour, 1997).

The model predictions for binary adsorption on Norit carbon are not as good as that for Ajax carbon, as shown in Figures 4 and 7, while the pore-size distribution of both carbons, as well as the conditions at which the pure component

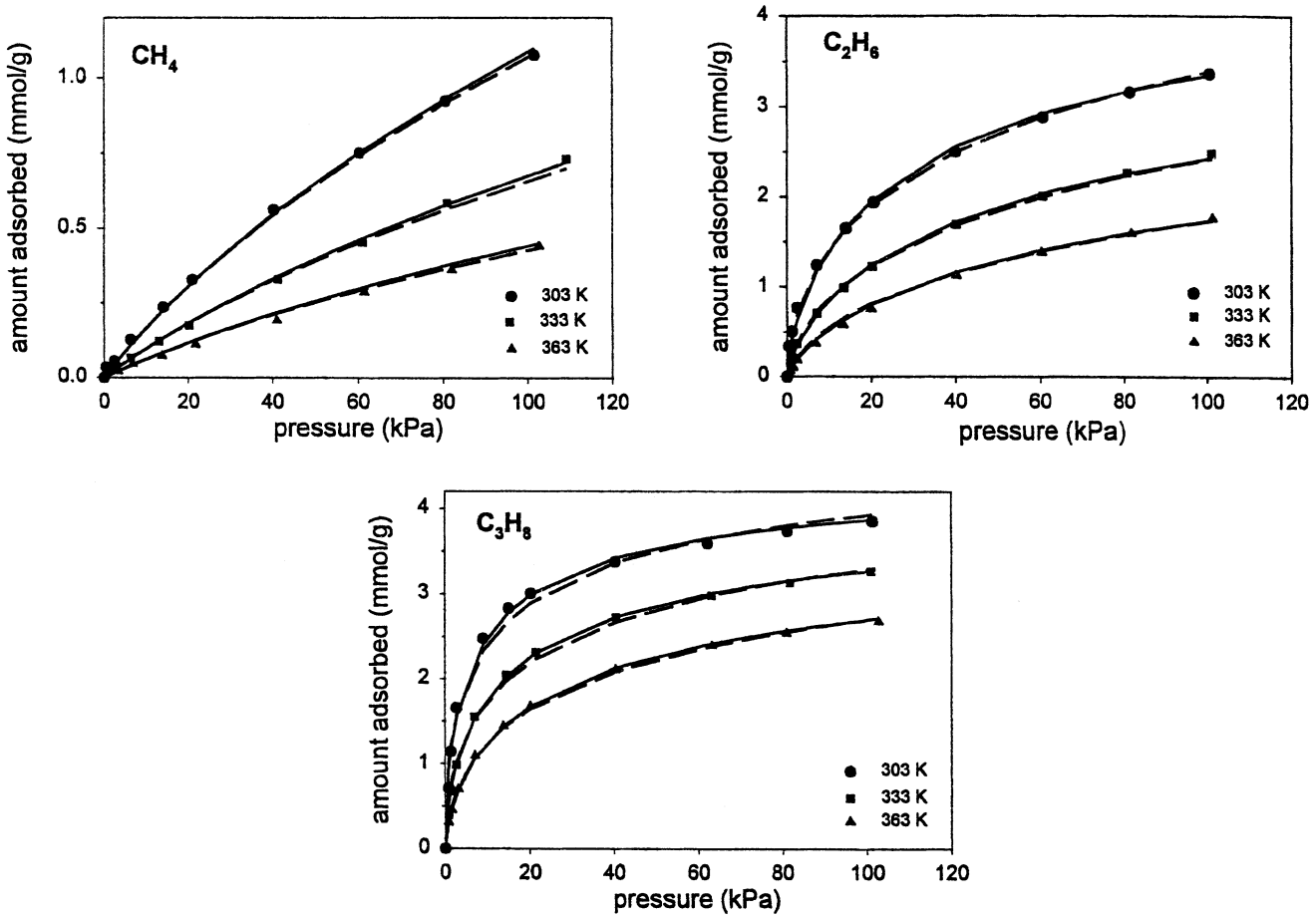

Figure 5. Adsorption isotherms on Norit carbon.

Solid lines are the fitting results using the present model, and dashed lines are results using the heterogeneous unmodified VST model. Symbols represent experimental data.

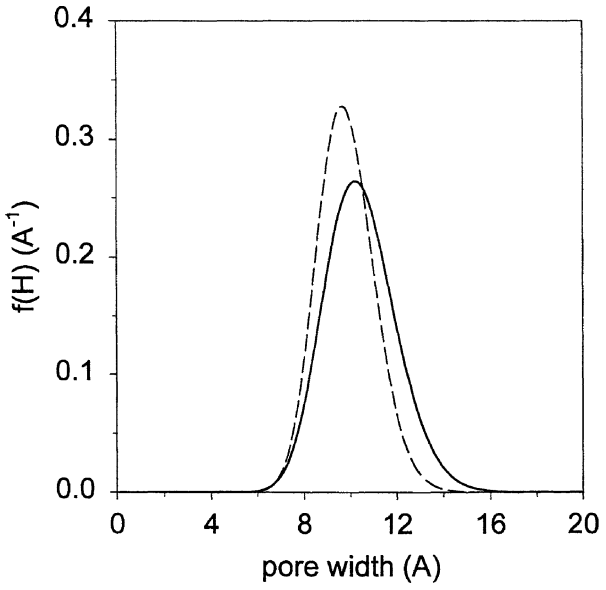

Figure 6. Micropore-size distribution of Norit carbon extracted by different models.

Solid line is the PSD from the present model, and dashed line is that from the heterogeneous unmodified VST model.

isotherms are measured, are similar. The greater deviation of the predictions for Norit carbon may be related to differences in the energetic heterogeneity of the adsorbent surfaces, beyond the structural heterogeneity considered here. In addition, deviation in structure from the one-dimensional slit-pore geometry with infinitely thick pore walls, assumed here, may contribute to the differences.

The prediction of binary adsorption equilibria on Norit carbon by the IAST-HMVST and IAST-HVST models were also performed, and the results are displayed in Figure 7 by the dotted and dashed lines, respectively. It can be seen that all three methods give very similar results for all the experimental conditions, indicating that large nonidealities are not of significance at the low-pressure involved, for the simple nonpolar hydrocarbons used. The deviation from the experimental data, as discussed earlier, however, does suggest the importance of energetic nonidealities.

Adsorption on Nuxit carbon

The single-component adsorption data of various hydrocarbons and CO_2 on Nuxit carbon at four different temperatures (Szepesy and Illes, 1963a,b) were fitted by this model. No information about the porous structure of this carbon is available. The micropore volume was therefore estimated from the PSD obtained by Davies and Seaton (2000) using a

Table 2. Parameters for Different Adsorptives on Norit Carbon

Adsorbate	σ_{ii} (nm)	$\delta_i \times 100$ (K^{-1})	ν_i^0	ϵ_{is} (kJ/mol)	q (nm^{-1})	γ	$n_{\nu\infty}$ ($mmol/cm^3$)
CH_4	0.38	0.793	1.025	7.597			
C_2H_6	0.39	0.402	1.336	12.428	45.03	46.0	16.07
C_3H_8	0.43	0.173	1.542	14.304			

Note: q, γ, and $n_{\nu\infty}$ are species-independent structural parameters.

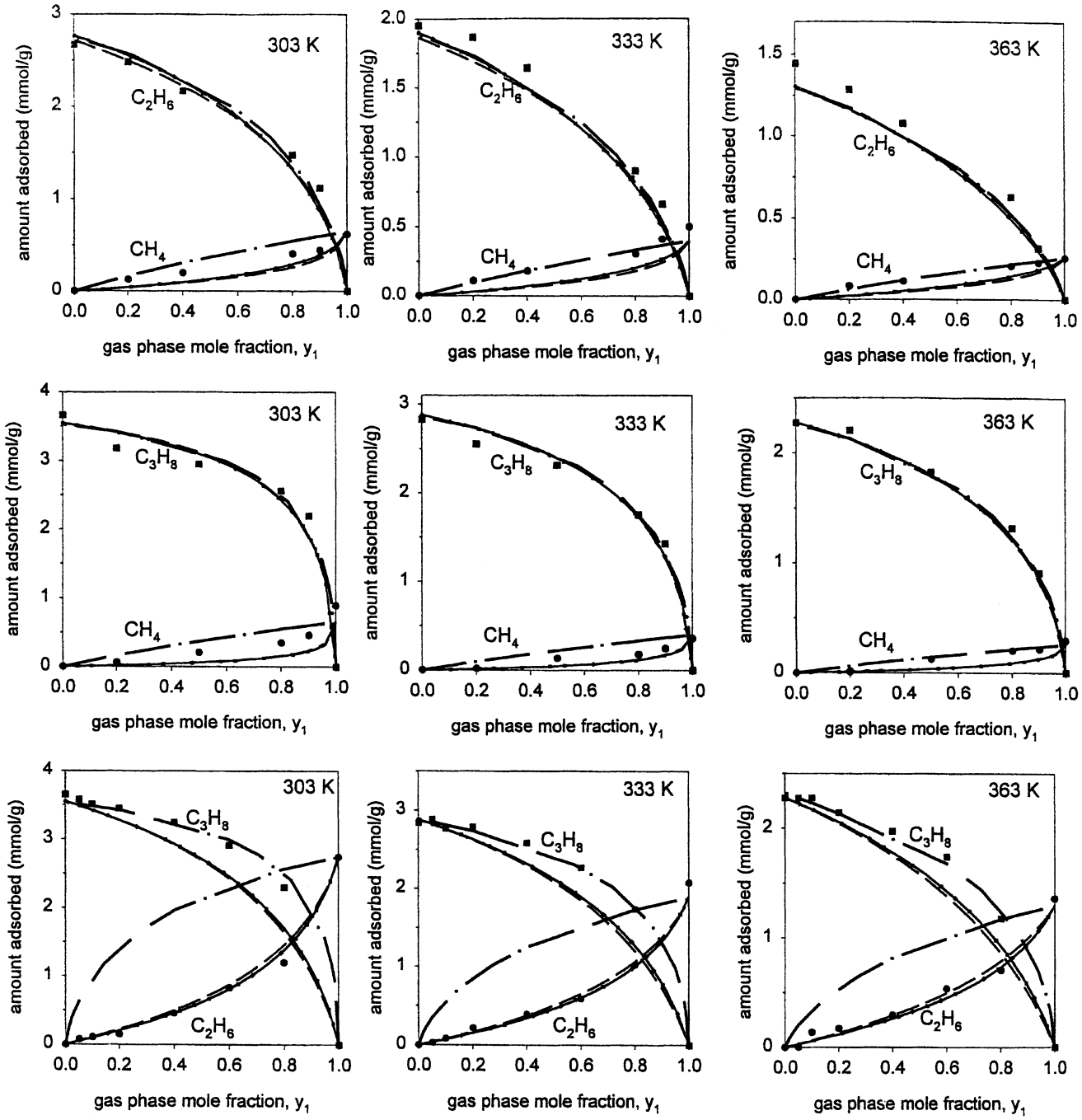

Figure 7. Prediction of binary adsorption equilibria on Norit carbon at bulk pressure of 50.6 kPa by different models.

Solid lines are results using the present model, dotted lines are results from the IAST-HMVST model, dashed lines are results of the IAST-HVST model. Dash-dotted lines are the single component isotherms at the corresponding partial pressure for each adsorbate. Symbols represent the experimental data.

molecular simulation interpretation of data for the adsorption of ethane at 293 K on Nuxit carbon, yielding its value as 0.38 cm^3/g.

The equilibrium model calculates the absolute adsorption, while the experiment measures the excess adsorption (Davies and Seaton, 1999), which is the absolute adsorption less the amount of adsorbate present in the adsorbent when no adsorption occurs. The absolute adsorption can be calculated from

$$n_i^a(P,T) = n_i^e(P,T) + \frac{\phi_i y_i P}{R_g T} V_p \qquad (22)$$

For the experimental data on Ajax and Norit carbons, the correction to the experimental excess isotherm was negligible at the low pressures used, and therefore it was not considered here. For adsorption on Nuxit carbon, however, the difference between absolute and excess adsorption, though small, could not be neglected at high pressures up to 6 atmosphere, and Eq. 22 was used in the calculation for adsorption on Nuxit carbon.

The values of the fitting parameters are listed in Table 3. The fitted isotherms are shown in Figure 8 as the solid lines, with the symbols representing the experimental data. The micropore-size distribution extracted from the calculation is depicted in Figure 9 by the solid line. Figure 9 shows that in the micropore range the PSD from this model is consistent with the result using molecular simulation (Davies and Seaton, 2000). Comparison of the calculated isotherms with the experiment also indicates that the proposed model can successfully correlate the experimental data over all temperatures. The heterogeneous unmodified VST model was also applied to the adsorption data on Nuxit carbon, and the dashed lines in Figure 8 represent the fitting results. The extracted micropore-size distribution by the HVST model is displayed in Figure 9 by the dashed line. Although the heterogeneous unmodified VST model can also fit the experimental data very well, it is not thermodynamically consistent, as indicated elsewhere (Ding and Bhatia, 2001).

The binary adsorption equilibria of eight pairs of components at 293 K and 101 kPa were subsequently predicted by the proposed model, and the resulting composition diagram is given in Figure 10 by the solid lines. All the predictions compare very well with the experimental data of Szepesy et al. (Szepesy and Illes, 1963c), again supporting the model as well as the accuracy of the fitting parameters. In addition, the IAST-HMVST and IAST-HVST model were also applied to predict the binary adsorption equilibria on Nuxit carbon, and the results are given in Figure 10 by the dotted and dashed lines, respectively. It can be seen that the heterogeneous modified VST model gives the best prediction, while another attractive feature of this method is that the calculation time using this method is much less than that using the IAST method. For example, the CPU time for CH_4 and C_2H_6 adsorption is only 30 s using the present model, while it is 650 s using the IAST-HMVST method. Although the improvement in computer speed may cause this difference to decrease in the near future, the benefit of the present model in terms of calculation time is indeed remarkable for the kinetic analysis of binary adsorption, with an improvement of more than an order of magnitude. It can be concluded that the proposed model for adsorption on activated carbon is an effective alternative for the prediction of binary adsorption equilibria. The comparison of the model prediction from three methods demonstrates the significance of size nonideality for binary adsorption equilibria on heterogeneous carbon. The current method accounts for the adsorbate nonideality caused by the size difference of the adsorbate molecules, which is not considered by the IAST scheme (Sircar, 1995).

Adsorption on BPL carbon

The experimental data of Reich et al. (1980) for CH_4, C_2H_6, C_2H_4, and CO_2 on BPL carbon at pressures up to about 35 atmospheres at 260.2 K and 301.4 K were also evaluated by the proposed model. The successful prediction of binary adsorption equilibria at high pressure on BPL carbon presented a challenge in earlier equilibrium studies, possibly due to the special porous structure of this carbon. Seaton and coworkers have developed a multispace adsorption model by accounting for the nonuniformity of the adsorbed phase through an empirical parameter characteristic of the adsorbent (Gusev et al., 1996; Jensen and Seaton, 1996; Jensen et al., 1997). A molecular simulation method, together with a networked pore model, is also proposed for this problem (Gusev and O'Brien, 1998; Davies and Seaton, 2000).

The pressure involved in the experimental data for adsorption on BPL carbon is as high as 35 atmospheres; therefore, the absolute isotherm was used in the calculation. Since there is no report on the porous structure of BPL carbon, a sample was analyzed in our laboratory by argon adsorption at 87 K, using a Micromeritics Inc. ASAP 2010. The isotherm was interpreted using the Micromeritics density functional theory package to determine the pore volume and pore-size distribution. In this way the micropore volume was estimated to be about 0.32 cm^3/g for BPL carbon.

The fitting parameters obtained from the heterogeneous modified VST model are given in Table 4. Figure 11 depicts

Table 3. Parameters for Different Adsorptives on Nuxit Carbon

Adsorbate	σ_{ii} (nm)	$\delta_i \times 100$ (K^{-1})	ν_i^0	ϵ_{is} (kJ/mol)	q (nm^{-1})	γ	$n_{\nu\infty}$ (mmol/cm^3)
CH_4	0.38	0.603	1.305	6.439			
C_2H_6	0.39	0.302	1.321	10.364			
C_3H_8	0.43	0.207	1.588	13.014			
C_4H_{10}	0.43	0.118	1.98	15.993	30.08	29.68	23.19
C_2H_4	0.39	0.362	1.28	9.795			
C_3H_6	0.45	0.233	1.506	12.472			
C_2H_2	0.33	0.789	1.102	10.922			
CO_2	0.33	0.809	0.862	8.949			

Note: q, γ, and $n_{\nu\infty}$ are species-independent structural parameters.

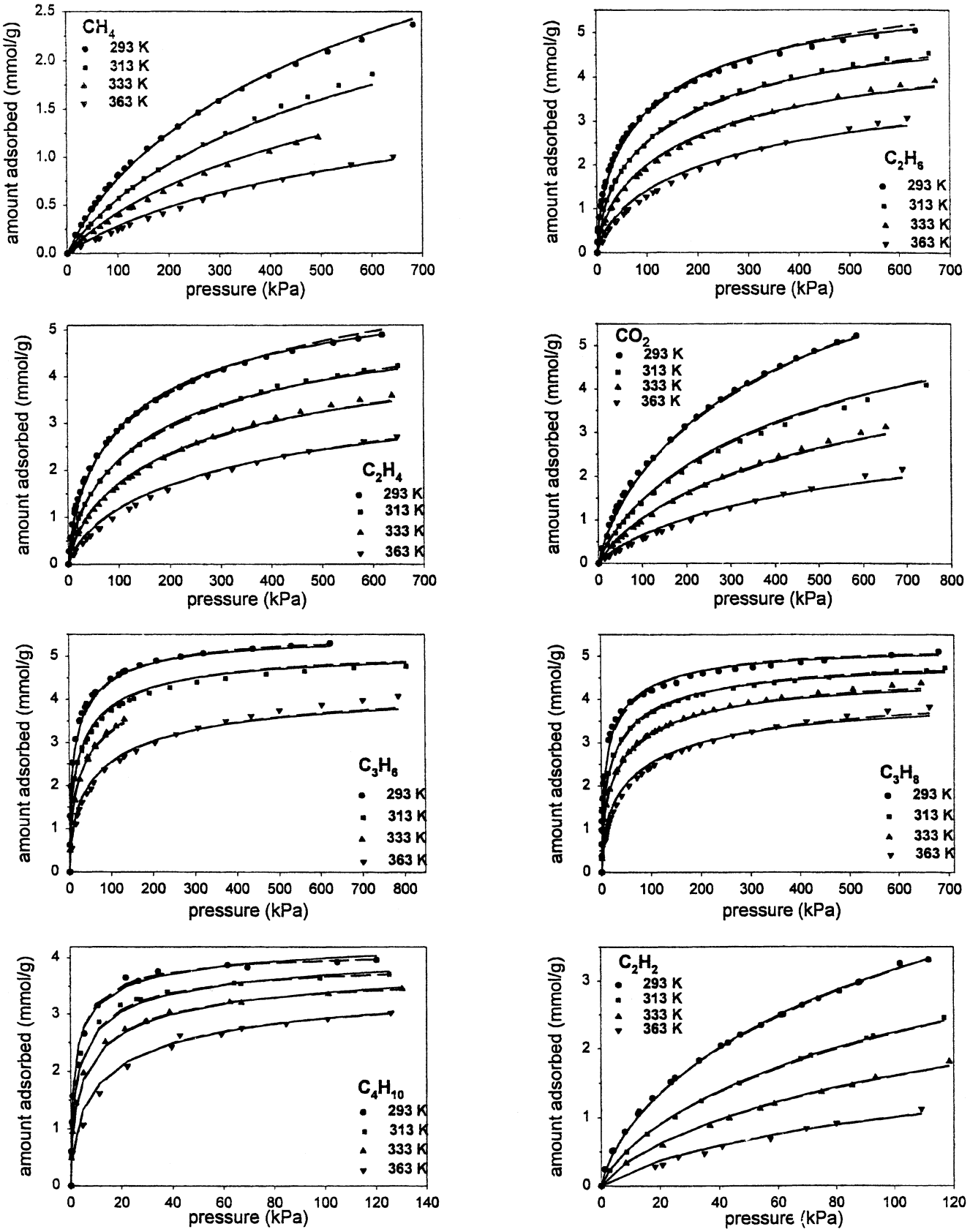

Figure 8. Adsorption isotherms on Nuxit carbon.

Solid lines are the fitting results using the present model, dashed lines are results using the heterogeneous unmodified VST model, and symbols represent experimental data.

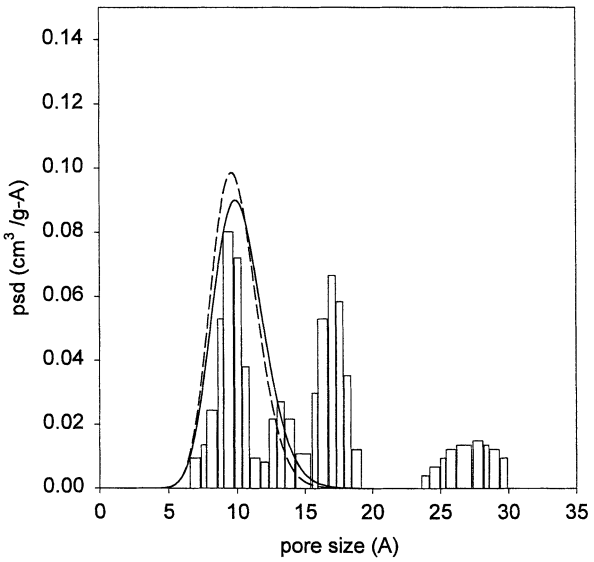

Figure 9. Pore-size distribution of Nuxit carbon obtained from different methods.

Solid line is the result from the present model, dashed line is the result from the heterogeneous unmodified VST model, and the bar plot is the molecular simulation-based result (from Davies and Seaton, 2000).

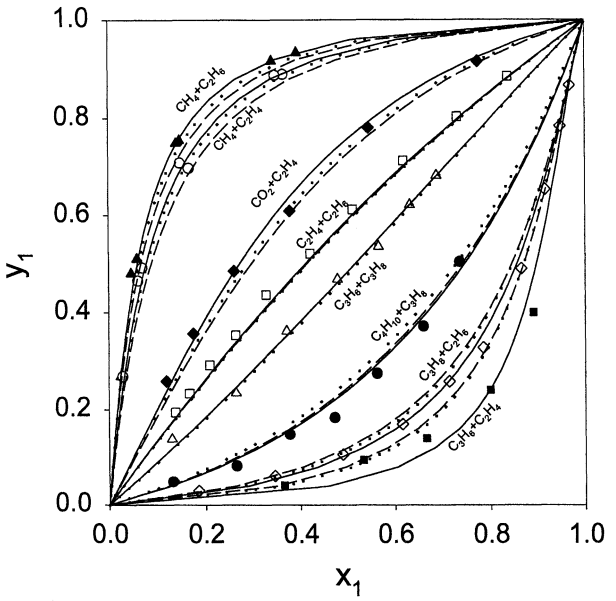

Figure 10. Predicted equilibrium diagrams and experimental data for binary adsorption on Nuxit carbon at 293 K and 101 kPa.

Solid lines are results from the present model, dotted lines are results using the IAST-HMVST model, and dashed lines are those from the IAST-HVST model. Symbols represent experimental data.

the fitted adsorption isotherms (solid lines) on BPL carbon along with the experimental data, indicating excellent agreement. The pore-size distribution obtained using this method is given in Figure 12 (the solid line), together with the DFT-based pore-size distribution from the ASAP measurement (dashed line). Because the DFT calculation result is given in terms of the physical pore width, which is the distance between the surfaces of the carbon molecules on opposite walls, it has been corrected by adding a carbon molecular size of 3.354 A to provide the center-to-center distance used in the abscissa of Figure 12. It is evident that the PSD extracted from the model fitting is consistent with the DFT result in the micropore range. Also shown in Figure 12 is the argon isotherm, given in the inset.

The parameters from fitting the single-component adsorption data were subsequently utilized to predict the binary adsorption equilibria for CH_4 and C_2H_4, as well as CH_4 and C_2H_6 at 301.4 K with different mole fractions. The predicted isotherms are shown in Figure 13 (solid lines), together with the experimental data. It can be seen that the model underpredicts the adsorption of CH_4 for all the cases, especially at higher operating pressure. The model prediction for the other compounds is in very good agreement with experiment.

One possible reason for the discrepancy in methane adsorption is the implicit assumption embedded in the model that the pores are bundled straight pores with complete accessibility. In other words, all the adsorbate molecules have equal accessibility to all the pores, which are simplified as the slit-shape voids confined by graphite layers. However, the real internal structure of activated carbon is far more complicated. First, the shape of the pores is irregular and there may be defects or constrictions in the pores. Second, the pattern of pore interconnections in the micropore network may lead to some of the pore space being inaccessible to some molecules due to size exclusion and percolation effects. While this behavior is quantitatively investigated for amorphous

Table 4. Parameters for Different Adsorptives on BPL Carbon Using Heterogeneous Modified VST Model

Adsorbate	σ_{ii} (nm)	$\delta_i \times 100$ (K^{-1})	ν_i^0	ϵ_{is} (kJ/mol)	q (nm^{-1})	γ	$n_{\nu\infty}$ (mmol/cm^3)
Unimodal Gamma Function							
CH_4	0.38	0.216	1.597	6.318			
C_2H_6	0.39	0.188	1.894	10.606	13.06	11.58	48.47
C_2H_4	0.39	0.201	1.788	9.778			
CO_2	0.33	0.399	1.153	8.16			
Known Bimodal Gamma Function with Different Accessible Pore Volume for Different Adsorbates							
CH_4	0.38	0.2	2.432	6.765			
C_2H_6	0.39	0.156	2.391	12.375			63.94
C_2H_4	0.39	0.167	2.364	11.313			
CO_2	0.33	0.347	1.872	8.991			

Note: q, γ, and $n_{\nu\infty}$ are species-independent structural parameters.

networks (López-Ramón et al., 1997; Ismadji and Bhatia, 2001), its influence for correlated networks is difficult to assess. This effect of such pore heterogeneity will be more evident for species with larger molecules, and also with increasing operation pressure. When the surface coverage is high, there will be more pores not available to bigger molecules. The effect of the pore heterogeneity may explain the discrepancy in the proposed model for binary equilibrium prediction on BPL carbon, as the difference in CH_4 adsorbed becomes more severe with increased pressure. Assuming such an effect, Davies and Seaton (1999) have empirically adjusted their model isotherms to allow for such inaccessible pore space for the larger molecule in mixtures with methane on BPL carbon. Utilizing a similar approach, the adsorption on BPL carbon may be represented by a modified expression as

$$n_{t,i}(P,T) = V_{p,i}\frac{n_{v\infty}}{v_i}\int_0^\infty \theta_i(H,P,T)f(H)\,dH, \qquad (23)$$

where $V_{p,i}$ is the species-dependent accessible pore volume.

Following Eq. 23 the fitting of both single and binary adsorption equilibrium data was performed simultaneously to estimate the value of $V_{p,i}$ for C_2H_4 and C_2H_6. For smaller molecules like CH_4 and CO_2, the value of total micropore volume is used as before. The results of individual accessible pore volume for C_2H_4 and C_2H_6 are 0.243 cm^3/g and 0.227 cm^3/g, respectively, indicating that about 25% of the total pore volume is not available to these molecules. The single and binary adsorption isotherms obtained by this method are plotted in Figures 11 and 13 as the dotted lines for comparison with the results from the original model prediction. The pore-size distribution is also given in Figure 12 by the dotted line. It can be seen that the result for single-component adsorption is comparable to when the original method is used, while the binary adsorption equilibrium prediction is significantly improved by this method. This observation supports the assumption that pore heterogeneity plays a role in adsorption equilibrium, especially at high pressures.

The pore-size distribution given in Figure 12 clearly shows a bimodal pore structure for BPL carbon according to DFT analysis of the argon adsorption isotherm. However, this can-

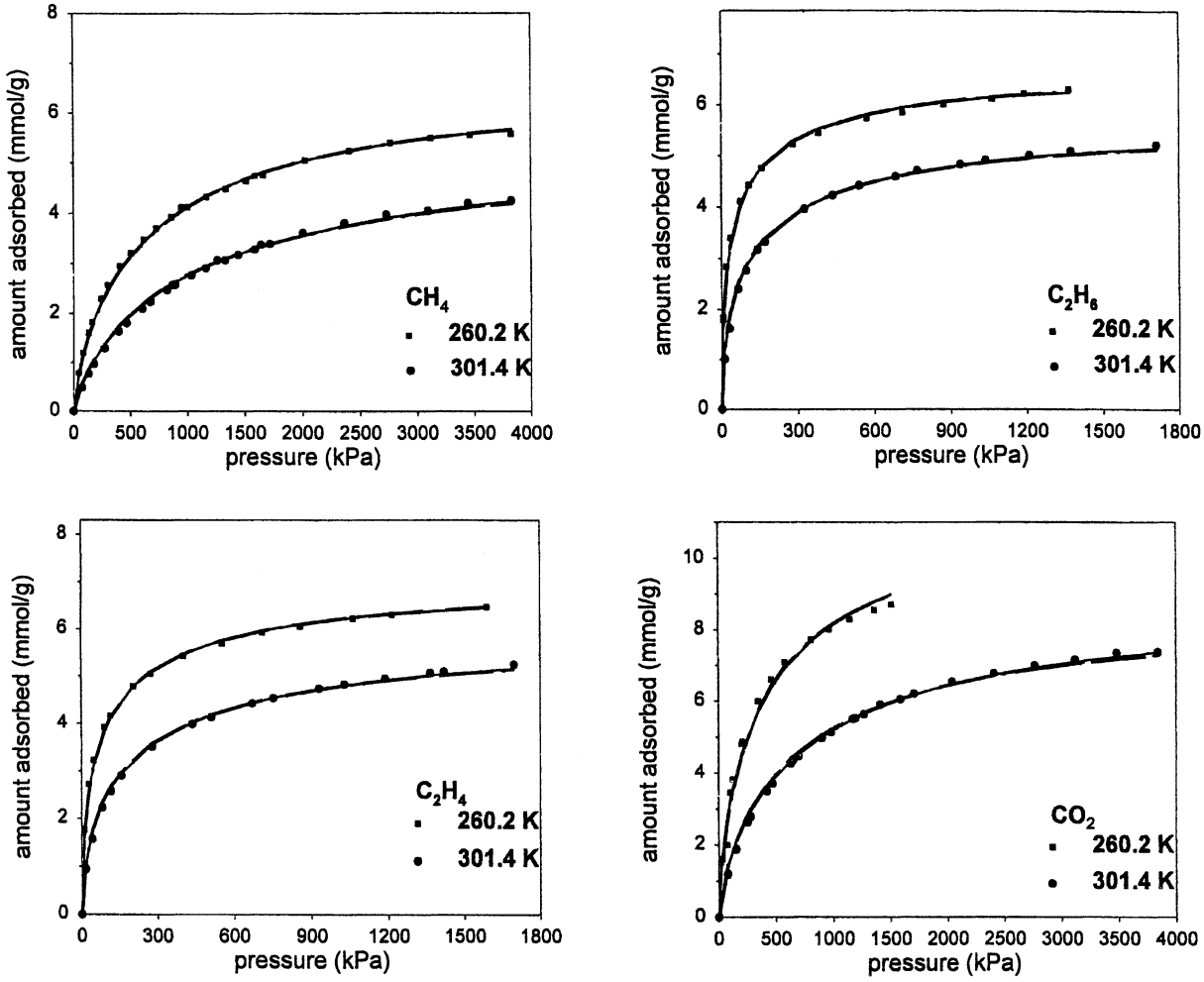

Figure 11. Adsorption isotherms on BPL carbon.

Solid lines are results using unimodal PSD with the same accessible volume for every adsorbate, dotted lines are results using unimodal PSD with different accessible pore volume for every adsorbate, dashed lines are results using bimodal PSD with the same accessible pore volume for each component, and dash-dotted lines are results using bimodal PSD and different accessible pore volume for each gas.

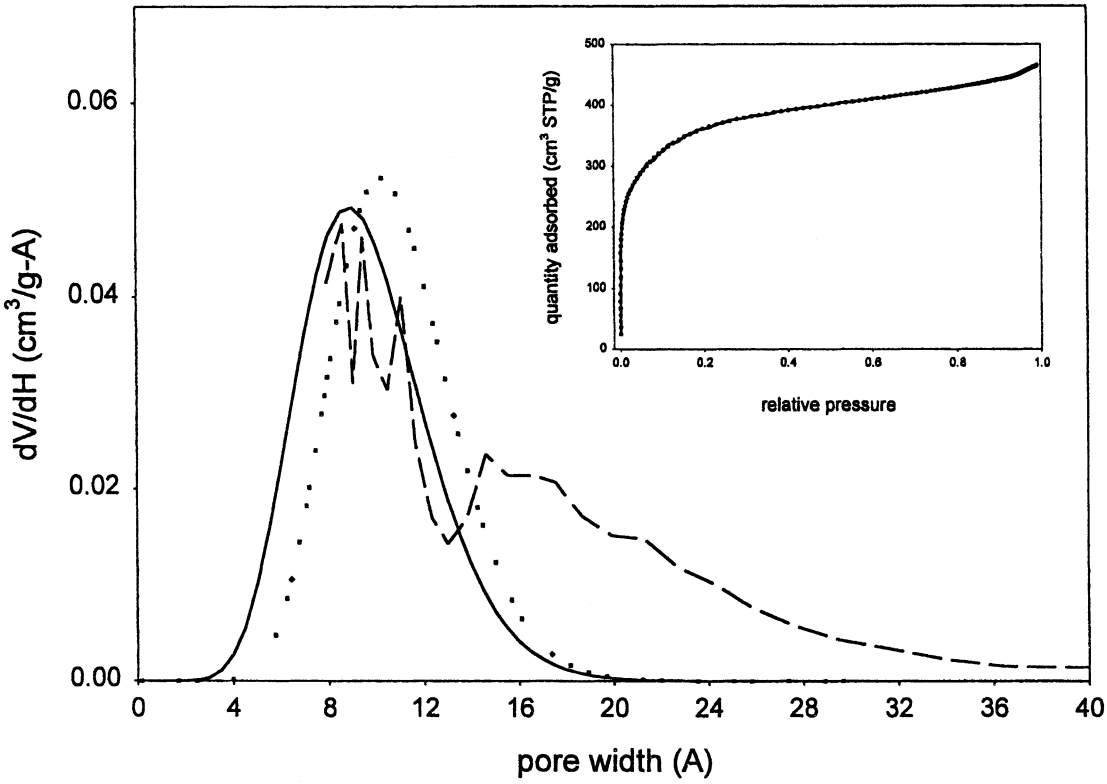

Figure 12. Pore-size distribution of BPL carbon compared with DFT result.

The solid line is the unimodal gamma function obtained from the present model with the same pore volume for every adsorbate, dotted line is the result with different pore volume for each component, and dashed line is the DFT-based PSD from argon adsorption. The inset is argon adsorption isotherm at 87 K.

not be represented by the model when a unimodal gamma distribution function is assumed. The simplification of the pore-size distribution may have little impact on adsorption at low pressures when the surface coverage is very low, and the adsorption predominantly occurs in smaller micropores contained within the unimodal gamma distribution function. However, assumption of unimodal PSD may cause some deviation in the calculated adsorption at very high pressures. Fitting the adsorption isotherms on BPL carbon while utilizing a bimodal gamma distribution function gave difficulty because of the larger number of parameters involved. Therefore, the PSD obtained from DFT interpretation of argon adsorption was used to correlate the single-component isotherms, by first fitting it by a smooth bimodal distribution curve. With the pore-size distribution fixed, the single-component isotherms were fitted by the proposed model with the same pore volume for all compounds. The results are given in Figure 11 by the dashed lines, demonstrating good fit. However, the binary adsorption equilibria subsequently predicted with the bimodal PSD, given in Figure 13 by the dashed lines, were similar to those using the unimodal PSD, suggesting that mesopore adsorption on this carbon does not contribute significantly in the pressure range used. Finally, the single-component as well as binary adsorption data on BPL carbon were also fitted with fixed bimodal PSD (from DFT) with variable accessible pore volume for each adsorbate. The fitted single- and binary-component adsorption isotherms are given in Figures 11 and 13 as the dash-dotted lines. The fitting parameters are listed in Table 4b. The excluded pore fraction in the result is about 25 and 30% of the total pore volume for C_2H_4 and C_2H_6, respectively. It can be seen that this approach can fit with the experimental data for single-component adsorption in comparison with the other three approaches, but this method gives more accurate prediction for binary adsorption. It can be concluded that the fitting result for single-component adsorption is not very sensitive to the pore-size distribution, but the pore-structure model is important for the accurate prediction of binary adsorption on heterogeneous carbon. The comparison of binary predictions by different models in Figure 13 suggests that the inclusion of binary adsorption data over a wide pressure range is more useful in examining the applicability of an equilibrium model. Of course, high pressures can lead to greater adsorbate–adsorbate interactions and deviations from the present model, which does not consider such interactions, so that an appropriate pressure range may need to be selected. However, the pore-structure model is generally not known *a priori*, and modifications to the assumed model may need to be made based on binary equilibrium predictions.

Physical significance of fitting parameters

Nonideality Parameter ν_i^0. The nonideality parameter, ν_i^0, may be expected to be closely related to the size of the adsor-

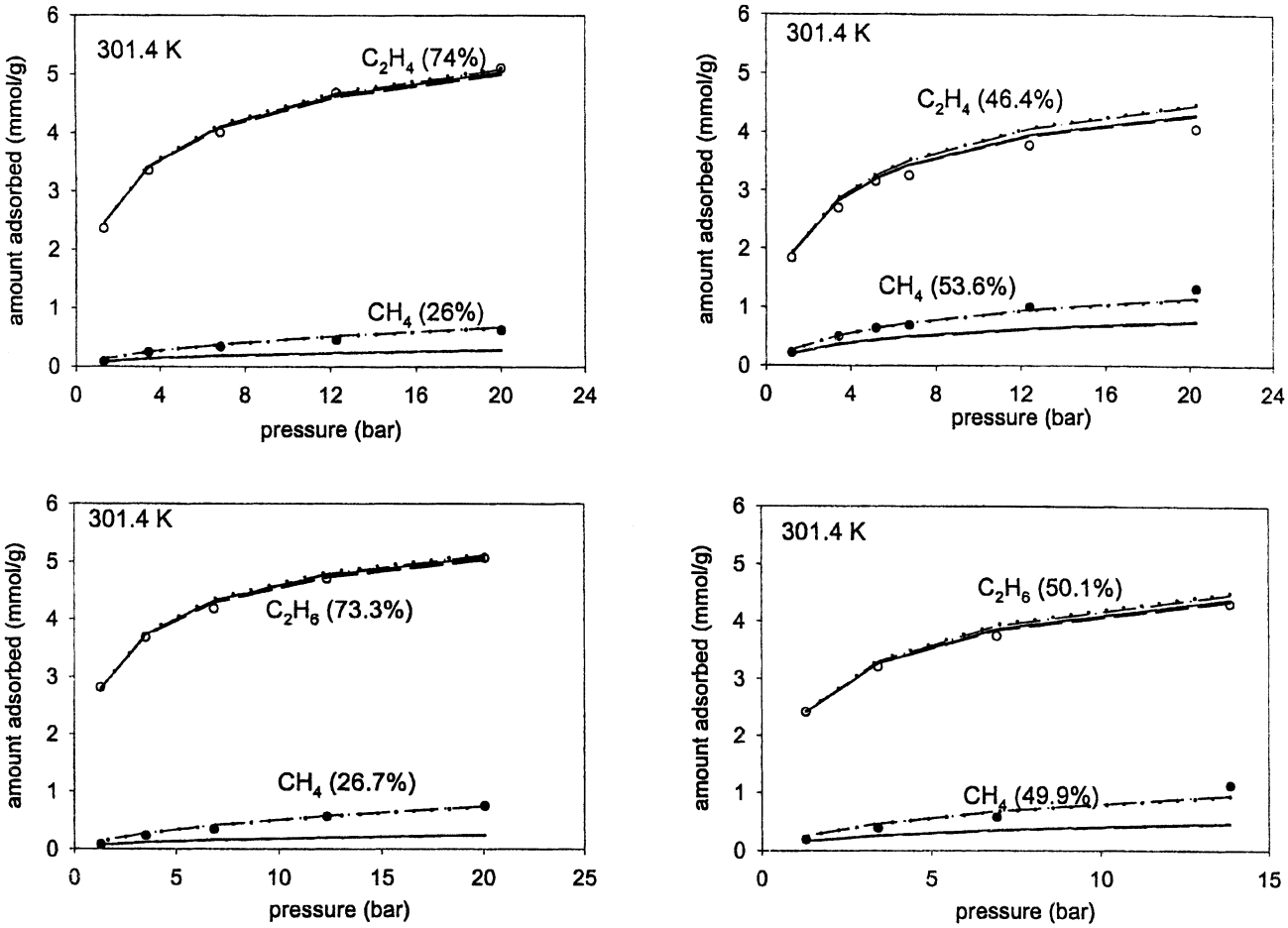

Figure 13. Prediction of binary adsorption equilibrium on BPL carbon.

Symbols represent experiment results, solid lines are results using unimodal PSD and the same accessible pore volume for every adsorbate, dotted lines represent results using unimodal PSD and different accessible pore volume for every adsorbate, dashed lines are results using bimodal PSD with the same accessible pore volume for each adsorbate, while dashed-dotted lines are results using known bimodal PSD with different pore volume for every component.

bate molecule, following

$$\nu_i^0 \propto \sigma_{ii}^n, \tag{24}$$

where σ_{ii} is the molecular size and n represents the dimension of the adsorbate packing. The value of n and the size of the vacant site can be estimated from Eq. 24 by plotting the fitting result for ν_i^0 vs. σ_{ii}, as given in Figure 14. The former is obtained as the slope of the correlation on logarithmic coordinates, while the latter is obtained from the value of σ_{ii} when $\nu_i^0 = 1$ (i.e., $\alpha_{i\nu} = 0$, following Eq. 11). It can be seen from the plot that the values of ν_i^0 for the adsorbates on Ajax and Norit carbon are close to each other, while the ones for BPL carbon are much larger, and those on Nuxit carbon are in between. For the adsorbates on Ajax and Norit carbon, the vacancy size is estimated at about 0.36 nm, with n estimated to be about 3. For adsorbates on Nuxit carbon, the vacancy size is about 0.33 nm with n estimated to be about 2.2. For adsorbates on BPL carbon, the vacancy is smaller and the size estimated to be about 0.21 nm. The decrease in vacancy size for the BPL carbon may possibly be related to the higher pressures used, and may be a more accurate figure, as near-saturation is achieved for some of the adsorbates. In addition, the value of 0.21 nm is also close to the value of 0.25 nm for the size of the potential well on a graphite plane, which supports this lower value. These results would suggest the importance of high-pressure data in isotherm fitting for gaseous adsorption.

For low pressures on Ajax and Norit carbon, the adsorbate molecule can locate randomly inside the pore in three dimensions, with the value of n close to 3. The dimension of the vacant site is in the magnitude of carbon molecular size. With the increase in pressure as for Nuxit and BPL carbon, the adsorbate molecules become closer to each other and have to be packed in an ordered way in two dimensions, or in a layer-by-layer way, with n becoming close to 2.

Solid–Fluid Interaction Parameter ϵ_{is}. The fitting results of ϵ_{is} by the proposed model for the adsorbates on different carbons are displayed in Figure 15. The result for adsorbates on Nuxit carbon is compared with that of the same species on

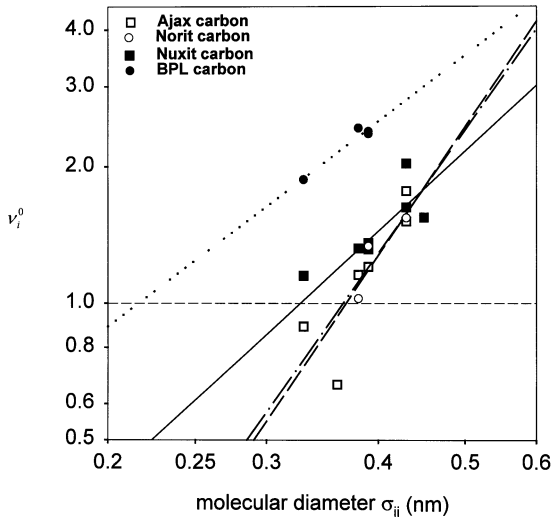

Figure 14. Variation of nonideality parameter ν_i^0 with molecular diameter for the adsorbates studied on four carbons.

The correlation of the results on Nuxit, Ajax, BPL, and Norit carbon are represented by the solid, dashed, dotted, and dashed-dotted lines, respectively.

the other three carbons. It is appropriate to say that the results are consistent on different carbons, although there is small difference between the values on different carbons, possibly due to the functional groups or impurities on the carbon surface.

Thermal Expansion Coefficient δ_i. In general, the values of δ_i are in a range appropriate for organic compounds (Lide, 2000). The fitting results for thermal expansion coefficient, δ_i, of all adsorbates on four carbons are compared in Figure 16. It is found that δ_i can be correlated with the molecular weight of the adsorbate by the following expression

$$\delta_i = A + \frac{B}{M_i}, \tag{25}$$

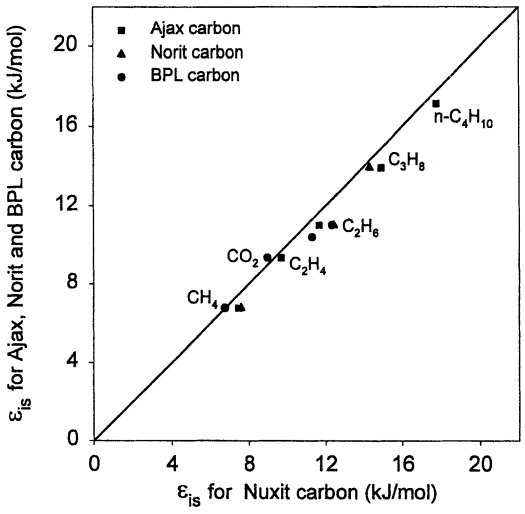

Figure 15. Comparison of fitting results of ϵ_{is} on various carbons.

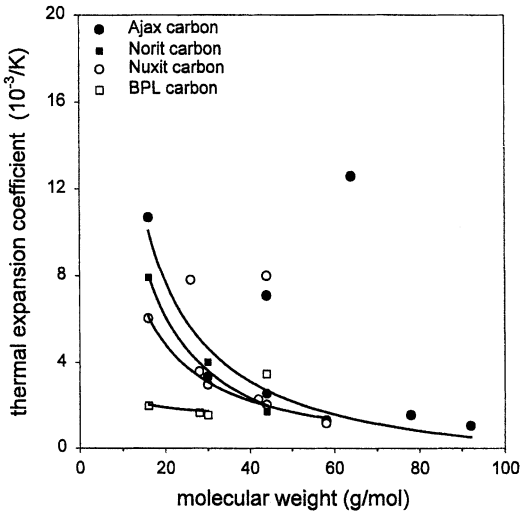

Figure 16. Comparison of thermal expansion coefficient δ_i on various carbons.

except the polar gases CO_2 and SO_2, and C_2H_2. For the Ajax and Norit carbons the results are similar, while those for the Nuxit carbon are slightly lower, and those for the BPL carbon are considerably lower. This is also the order of the maximum pressure for the data, with the Ajax and Norit data corresponding to slightly subatmospheric pressures, and the Nuxit and BPL data having maximum pressures of about 6 bar and 35 bar, respectively. With an increase in pressure, the value of the thermal expansion coefficient may be expected to decrease significantly for the supercritical and nonideal gaseous phases, as is indeed observed. This suggests that δ_i may be considered dependent on the pressure or chemical potential in the model, but this is a second-order effect, given the small values of δ_i.

Conclusions

A heterogeneous modified vacancy solution model is investigated for adsorption equilibrium on porous solids. The model was successfully applied to the single- and binary-adsorption equilibrium data on four different activated carbons for various components at multiple temperatures under a wide range of pressures. For the single-component data studied, the model can fit all the experimental data very well, and the micropore-size distribution extracted from the proposed model is reasonable. The fitting results for the size nonideality parameter, ν_i^0, for the adsorbates on different carbons are consistent with the pressure change and can be correlated with the molecular size. The values of fitting parameter, ϵ_{is}, obtained are also consistent for the same adsorbate on different carbons. It is found that the proposed model can predict binary adsorption equilibria somewhat better than the IAST method does, confirming the significance of the nonideality parameter, ν_i^0, accounting for the size difference between adsorbates. While the proposed model is an effective and efficient approach for the prediction of binary adsorption equilibria on heterogeneous carbons, further improvements can be made by considering energetic nonidealities, neglected in the Flory–Huggins approach utilized.

Acknowledgment

This research has been supported by a grant from the Australian Research Council under the Large Research Grants Scheme.

Notation

H = pore width
$H_{i,\min}$ = minimum micropore width accessible to species i
K_i = Henry's law constant
M = molecular weight
n = constant representing molecular packing shape on vacancy
n_i = amount adsorbed
$n_{v\infty}$ = saturation capacity of vacant site
P = pressure
q = gamma distribution function parameter
R_g = universal gas constant
S_{12} = binary selectivity
T = temperature
T_0 = reference temperature, 273 K
X_i^a = mole fraction of component i
y_i = mole fraction of component i in the bulk phase
$V_{p,i}$ = pore volume to component i
z = perpendicular distance from a surface plane of pore

Greek letters

α_{ij} = Flory-Huggins interaction parameter between i and j
δ_i = thermal expansion coefficient
Φ_{mi} = minimum potential energy in micropore of width H
ϕ_{is} = interaction energy of a molecule with one side of the micropore wall
ϕ_i^g = bulk fugacity coefficient
γ = gamma function parameter
γ_i^a = activity of component i
ν_i = site occupancy of one adsorbate molecule
ν_i^0 = site occupancy at reference temperature T_0
θ_i = fractional coverage on vacant sites
ρ_s = surface number density of carbon atoms in a graphite layer
σ_{ii} = hard-sphere diameter
σ_{is} = solid–fluid LJ collision diameter calculated by the Lorentz rule
Δ = separation between graphite layers
ϵ_{is} = solid–fluid interaction well

Literature Cited

Ahmadpour, A., "Fundamental Studies on Preparation and Characterization of Carbonaceous Adsorbents for Natural Gas Storage," PhD Thesis, The Univ. of Queensland, Brisbane, Australia (1997).

Assael, M. J., T. F. Tsolakis, and J. P. M. Trusler, *Thermophysical Properties of Fluids: An Introduction to Their Prediction*, Imperial College Press, London (1996).

Bhatia, S. K., "Adsorption of Binary Hydrocarbon Mixtures in Carbon Slit Pores—A Density Functional Theory Study," *Langmuir*, **14**, 6231 (1998).

Bhatia, S. K., and L. P. Ding, "The Vacancy Solution Theory of Adsorption Revisited," *AIChE J.*, **47**, 2136 (2001).

Cochran, T. W., R. L. Kabel, and R. P. Danner, "Vacancy Solution Theory of Adsorption Using Flory-Huggins Activity Coefficient Equations," *AIChE J.*, **31**, 268 (1985a).

Cochran, T. W., R. L. Kabel, and R. P. Danner, "Vacancy Solution Theory of Adsorption—Improvements and Recommendations," *AIChE J.*, **31**, 2075 (1985b).

Davies, G. M., and N. A. Seaton, "Development and Validation of Pore Structure Models for Adsorption in Activated Carbons," *Langmuir*, **15**, 6263 (1999).

Davies, G. M., and N. A. Seaton, "Predicting Adsorption Equilibrium Using Molecular Simulation," *AIChE J.*, **46**, 1753 (2000).

Ding, L. P., and S. K. Bhatia, "Application of Heterogeneous Vacancy Solution Theory to Characterization of Microporous Solids," *Carbon*, **39**, 2215 (2001).

Ding, L. P., S. K. Bhatia, and F. Liu, "Kinetics of Adsorption on Activated Carbon: Application of Heterogeneous Vacancy Solution Theory," *Chem. Eng. Sci.* (2002).

Do, D. D., and H. D. Do, "A New Adsorption Isotherm for Heterogeneous Adsorbent Based on the Isosteric Heat as a Function of Loading," *Chem. Eng. Sci.*, **52**, 297 (1997).

Do, D. D., and K. Wang, "Dual Diffusion and Finite Mass Exchange Model for Adsorption Kinetics in Activated Carbon," *AIChE J.*, **44**, 68 (1998).

Fowler, R. H., and E. A. Guggenheim, *Statistical Thermodynamics: A Version of Statistical Mechanics for Students of Physics and Chemistry*, Cambridge Univ. Press, Cambridge (1949).

Gusev, V., and J. A. O'brien, "Prediction of Gas Mixture Adsorption on Activated Carbon Using Molecular Simulations," *Langmuir*, **14**, 6328 (1998).

Gusev, V., J. A. O'brien, C. R. C. Jensen, and N. A. Seaton, "Theory for Multicomponent Adsorption Equilibrium—Multispace Adsorption Model," *AIChE J.*, **42**, 2773 (1996).

Hill, T. L., *An Introduction to Statistical Thermodynamics*, Addison-Wesley, Reading, MA (1960).

Ismadji, S., and S. K. Bhatia, "Characterization of Activated Carbons Using Liquid Phase Adsorption," *Carbon*, **39**, 1237 (2001).

Jaroniec, M., J. Choma, A. Swiatkowski, and K. H. Radeke, "Application of Isotherm Equation Associated with Gamma Micropore-Size Distribution for Characterizing Activated Carbons," *Chem. Eng. Sci.*, **43**, 3151 (1988).

Jensen, C. R. C., and N. A. Seaton, "An Isotherm Equation for Adsorption to High Pressures in Microporous Adsorbents," *Langmuir*, **12**, 2866 (1996).

Jensen, C. R. C., N. A. Seaton, V. Gusev, and J. A. O'brien, "Prediction of Multicomponent Adsorption Equilibrium Using a New Model of Adsorbed Phase Nonuniformity," *Langmuir*, **13**, 1205 (1997).

Kierlik, E., and M. L. Rosinberg, "Density-Functional Theory for Inhomogeneous Fluids: Adsorption of Binary Mixtures," *Phys. Rev. A*, **44**, 5025 (1991).

Langmuir, I., "The Adsorption of Gases on Plane Surfaces of Glass, Mica and Platinum," *J. Amer. Chem. Soc.*, **40**, 1361 (1918).

Lide, D. R., *Handbook of Chemistry and Physics*, CRC Press, Boca Raton, FL (2000).

López-Ramón, M. V., J. Jagiello, T. J. Bandosz, and N. A. Seaton, "Determination of the Pore Size Distribution and Network Connectivity in Microporous Solids by Adsorption Measurements and Monte Carlo Simulation," *Langmuir*, **13**, 4435 (1997).

McEnaney, B., "Estimation of the Dimensions of Micropores in Active Carbons Using the Dubinin-Radushkevich Equation," *Carbon*, **25**, 69 (1987).

Myers, A. L., and J. M. Prausnitz, "Thermodynamics of Mixed-Gas Adsorption," *AIChE J.*, **11**, 121 (1965).

Nitta, T., T. Shigetomi, M. Kuro-Oka, and T. Katayama, "An Adsorption Isotherm of Multi-Site Occupancy Model for Homogeneous Surface," *J. Chem. Eng. Jpn.*, **17**, 39 (1984).

Olivier, J. P., "Modeling Physical Adsorption on Porous and Nonporous Solids Using Density Functional Theory," *J. Porous Mater.*, **2**, 9 (1995).

Press, W. H., S. A. Teukolsky, W. T. Vetterling, and B. P. Flannery, *Numerical Recipes in Fortran: The Art of Scientific Computing*, Cambridge Univ. Press, Cambridge (1992).

Qiao, S., K. Wang, and X. Hu, "Study of Binary Adsorption Equilibrium of Hydrocarbons in Activated Carbon Using Micropore Size Distribution," *Langmuir*, **16**, 5130 (2000).

Rao, M. B., and S. Sircar, "Thermodynamic Consistency for Binary Gas Adsorption Equilibria," *Langmuir*, **15**, 7258 (1999).

Reich, R., W. T. Ziegler, and K. A. Rogers, "Adsorption of Methane, Ethane, and Ethylene Gases and Their Binary and Ternary Mixtures and Carbon Dioxide on Activated Carbon at 212-301 K and Pressures to 35 Atmospheres," *Ind. Eng. Chem. Process Des. Dev.*, **19**, 336 (1980).

Sircar, S., "Influence of Adsorbate Size and Adsorbent Heterogeneity on IAST," *AIChE J.*, **41**, 1135 (1995).

Somers, S. A., A. V. Mccormick, and H. T. Davis, "Superselectivity and Solvation Forces of a Two Component Fluid Adsorbed in Slit Micropores," *J. Chem. Phys.*, **99**, 9890 (1993).

Steele, W. A., "The Physical Interaction of Gases with Crystalline Solids," *Surf. Sci.*, **36**, 317 (1973).

Suwanayuen, S., and R. P. Danner, "A Gas Adsorption Isotherm Equation Based on Vacancy Solution Theory," *AIChE J.*, **26**, 68 (1980a).

Suwanayuen, S., and R. P. Danner, "Vacancy Solution Theory of Adsorption from Gas Mixtures," *AIChE J.*, **26**, 76 (1980b).
Szepesy, L., and V. Illes, "Adsorption of Gases and Gas Mixtures, I. Measurement of the Adsorption Isotherms of Gases on Active Carbon up to Pressures of 1000 Torr," *Acta Chim. Hung.*, **35**, 37 (1963a).
Szepesy, L., and V. Illes, "Adsorption of Gases and Gas Mixtures, II. Measurement of the Adsorption Isotherms of Gases on Active Carbon under Pressures of 1 to 7 Atm," *Acta Chim. Hung.*, **35**, 53 (1963b).
Szepesy, L., and V. Illes, "Adsorption of Gases and Gas Mixtures, III. Investigation of the Adsorption Equilibria of Binary Gas Mixtures," *Acta Chim. Hung.*, **35**, 245 (1963c).
Talu, O., and A. L. Myers, "Letter to the Editor," *AIChE J.*, **34**, 1931 (1988).
Wang, K., "The Effect of Microporous Structure on Adsorption Equilibria and Kinetics on Activated Carbon," PhD Thesis, The Univ. of Queensland, Brisbane, Australia (1998).
Yang, R. T., *Gas Separation by Adsorption Processes*, Imperial College Press, London (1997).

Manuscript received Aug. 20, 2001, and revision received Feb. 13, 2002.